Lidocaine Inhibits HCN Currents in Rat Spinal Substantia Gelatinosa Neurons

Tao Hu, MD,*† Nana Liu, MD,* Minhua Lv, MD,‡ Longxian Ma, MD,† Huizhen Peng, MD,† Sicong Peng,* and Tao Liu, PhD, MD*

BACKGROUND: Lidocaine, which blocks voltage-gated sodium channels, is widely used in surgical anesthesia and pain management. Recently, it has been proposed that the hyperpolarization-activated cyclic nucleotide (HCN) channel is one of the other novel targets of lidocaine. Substantia gelatinosa in the spinal dorsal horn, which plays key roles in modulating nociceptive information from primary afferents, comprises heterogeneous interneurons that can be electrophysiologically categorized by firing pattern. Our previous study demonstrated that a substantial proportion of substantia gelatinosa neurons reveal the presence of HCN current (I_h); however, the roles of lidocaine and HCN channel expression in different types of substantia gelatinosa neurons remain unclear.

METHODS: By using the whole-cell patch-clamp technique, we investigated the effect of lidocaine on I_h in rat substantia gelatinosa neurons of acute dissociated spinal cord slices.

RESULTS: We found that lidocaine rapidly decreased the peak I_h amplitude with an IC_{50} of 80 μM. The inhibition rate on I_h was not significantly different with a second application of lidocaine in the same neuron. Tetrodotoxin, a sodium channel blocker, did not affect lidocaine's effect on I_h. In addition, lidocaine shifted the half-activation potential of I_h from −109.7 to −114.9 mV and slowed activation. Moreover, the reversal potential of I_h was shifted by −7.5 mV by lidocaine. In the current clamp, lidocaine decreased the resting membrane potential, increased membrane resistance, delayed rebound depolarization latency, and reduced the rebound spike frequency. We further found that approximately 58% of substantia gelatinosa neurons examined expressed I_h, in which most of them were tonically firing.

CONCLUSIONS: Our studies demonstrate that lidocaine strongly inhibits I_h in a reversible and concentration-dependent manner in substantia gelatinosa neurons, independent of tetrodotoxin-sensitive sodium channels. Thus, our study provides new insight into the mechanism underlying the central analgesic effect of the systemic administration of lidocaine. (Anesth Analg 2016;122:1048–59)

Lidocaine is one of the most widely used local anesthetics in surgical anesthesia and in the management of acute postoperative and chronic pain syndromes.[1–3] Its anesthetic action is typically produced by blocking voltage-gated sodium channels that are responsible for neuronal signal propagation.[4] Moreover, increasing evidence has indicated that lidocaine affects other channels such as calcium channels,[5–7] potassium channels,[8–11] and transient receptor potential channels.[12–15] Recently, the hyperpolarization-activated cyclic nucleotide (HCN) channel has been identified as a novel target of lidocaine.[16–19]

HCN channel family (HCN1–4)–mediated current (I_h) is a slowly activated, mixed inward current carried by Na+ and K+.[20,21] Diverse functions of I_h have been described, including modulation of the resting membrane potential (RMP), action potential firing frequency, neuronal network oscillation, and dendritic integration.[22–25] These functions contribute to nociception, thalamocortical oscillations, and hippocampal plasticity. Recently, attention has been paid to the effect of the HCN channel on inflammatory, neuropathic, and postoperative pain. For instance, abundant axonal accumulation of HCN channels has been observed after nerve injury.[26–29] Concomitantly, systemic administration of ZD7288, a selective inhibitor of HCN channels, has been shown to significantly alleviate mechanical allodynia, likely because of the suppression of ectopic discharges in dorsal root ganglion (DRG) neurons.[30,31] In addition, *HCN1* gene knockout was observed to partially prevent the development of mouse cold allodynia.[32,33] Similarly, in HCN2 genetically deleted mice, neuropathic pain was inhibited because of reduced I_h currents and action potential firing rate.[34] These observations indicate that HCN channels are involved in pain generation and maintenance.

It has been reported that lidocaine can inhibit I_h in *Xenopus* oocytes,[18] DRG,[16,19] and thalamocortical neurons.[17] In both sciatic nerve block and intrathecal anesthesia experiments, the anesthetic durations of lidocaine in HCN1−/− mice has been observed to be shorter than that in wild-type mice.[16] Moreover, studies have shown that the anesthetic duration of lidocaine is prolonged by the coadministration of ZD7288.[16,35,36] In contrast, forskolin, a potent nonspecific adenylyl cyclase activator that can enhance I_h, has been

shown to reduce the pinprick blockade duration of lidocaine.[16] Therefore, it is possible that suppression of I_h could be another analgesic mechanism of lidocaine.

Rexed laminae II in the spinal dorsal horn, also referred to as the substantia gelatinosa (SG), integrates nociceptive information from the periphery to the brain and plays a crucial role in nociceptive transmission. Neuronal circuitry in the SG is complicated by a predominance of excitatory interneurons and can be classified according to discharge pattern.[37–40] Our previous study showed that a substantial proportion of SG neurons expresses the HCN channel.[41] Furthermore, it has been demonstrated that systemic administration of lidocaine can suppress spontaneous action potential firings of SG neurons, indicating that SG neurons may be affected by lidocaine through this route of administration.[42]

Given that HCN channels and spinal SG neurons play important roles in inflammatory and neuropathic pain, we hypothesize that lidocaine can block HCN channels in SG neurons. Thus, the aim of this study was to investigate the effect and molecular mechanisms of lidocaine on the HCN channel and to determine the HCN channel distribution in SG subtypes classified by discharge pattern.

METHODS
Preparation of Spinal Cord Slices
All experimental procedures were in accordance with protocols approved by the Institutional Animal Care and Use Committee of Nanchang University Guidelines. Spinal cord slices were prepared from male Sprague Dawley rats (3–5 weeks old) as described previously.[41,43] Briefly, rats deeply anesthetized with urethane (1.5 g/kg, intraperitoneally) were perfused transcardially with ice-cold carbogenated (95% O_2 and 5% CO_2) sucrose-substituted artificial cerebrospinal fluid (s-ACSF) containing the following (in millimolar): 240 sucrose, 2.5 KCl, 0.5 $CaCl_2$, 3.5 $MgCl_2$, 1.25 NaH_2PO_4, 25 $NaHCO_3$, 0.4 ascorbate acid, and 2 pyruvate. The lumbosacral spinal cord was immediately dissected and immersed in the same s-ACSF. Animals were then killed by decapitation after extraction and while still under anesthesia. Parasagittal slices measuring 300 µm in thickness were cut with a microslicer (VT1000S; Leica, Nussloch, Germany). The slices were incubated at 32°C for at least 30 minutes in normal carbogenated ACSF containing the following (in millimolar): 117 NaCl, 3.6 KCl, 2.5 $CaCl_2$, 1.2 $MgCl_2$, 1.2 NaH_2PO_4, 25 $NaHCO_3$, 11 D-glucose, 0.4 ascorbic acid, and 2 pyruvate (pH = 7.4).

Electrophysiologic Recordings
Whole-cell patch-clamp recordings were conducted as in our previous study.[41] After incubation, 1 spinal cord slice was transferred to a recording chamber and continuously perfused with ACSF (2–4 mL/min) at room temperature. The SG neurons in lumbar segments L4 to L5 were visualized with an IR-DIC camera (IR-1000; Dage, Michigan City, IN). Patch pipettes were pulled from the borosilicate glass (World Precision Instruments, Sarasota, FL) on a micropipette puller (P-97; Sutter Instrument, Novato, CA). Typical resistances ranged from 3 to 5 MΩ when filled with a solution containing the following (in millimolar): 130 K-gluconate, 5 KCl, 4 Mg-ATP, 10 phosphocreatinine, 0.5 EGTA, 0.3 Li-GTP, 10

HEPES (pH = 7.3, adjusted with KOH, 300 mOsm). Signals were amplified with an EPC-10 amplifier and Patchmaster software (HEKA Electronik, Lambrecht, Germany). Series resistances typically measured between 20 and 30 MΩ and were monitored throughout the recording period. Data were excluded if the series resistance changed by >20%. RMP was measured in the current clamp with no holding current.

Chemicals
All drugs were obtained from Sigma-Aldrich (St. Louis, MO), except for ZD7288 and tetrodotoxin (TTX), which were obtained from Tocris Bioscience (Bristol, UK). Lidocaine, ZD7288, and TTX were dissolved in distilled water at 1000 times the concentration to be used and stored at −20°C. Before application, these drugs were immediately diluted to the respective concentrations in ACSF solution.

Statistical Analysis
I_h currents and membrane voltage responses were analyzed using Patchmaster and GraphPad Prism 5.0 software (GraphPad Prism Software, Inc., La Jolla, CA). I_h is composed of an instantaneous (I_{inst}) and a steady-state component (I_{ss}).[44,45] The amplitude of I_h was calculated as the difference between I_{ss} and I_{inst} at the evoked voltage of −130 mV unless indicated otherwise. The current density was calculated by dividing the amplitude of I_h by the cell capacitance at every test potential.

To determine IC_{50}, a dose-dependent curve was fitted with the Hill equation as follows: $y = I_{max}/(1 + IC_{50}/x)$, where I_{max} represents the maximal current amplitude, IC_{50} is the half-maximal inhibitory concentration, and x is the concentration of lidocaine in micromolar.

To estimate $V_{0.5}$ (the voltage at which the current is one-half of its maximal level), the activation curves were fitted using GraphPad Prism with the Boltzmann sigmoidal equation: $I/I_{max} = 1/(1 + \exp[(V_{0.5} − V)/k]$, where I_{max} represents the maximal current amplitude, $V_{0.5}$ is the midpoint potential, V is the membrane potential, and k is the slope factor.

The time constant (τ) of I_h activation was obtained by fitting the current traces (from instantaneous to 500 milliseconds) with a single exponential equation as follows: $I_{(t)} = I_h \times \exp(−t/\tau) + I_{ss}$, where $I_{(t)}$ is the amplitude of the current at time t, I_h represents the current amplitude, and τ is the time constant.[46,47]

To determine the reversal potential (V_{rev}), the recorded tail current amplitudes during deactivation were plotted against each test potential to construct I-V curves. V_{rev} is the intersection of the I-V curve with the x-axis. The input resistance (R_{in}) was calculated based on the current change during a 10 mV hyperpolarizing pulse.

SPSS version 17.0 (SPSS Inc., Chicago, IL) was used for all the statistical analysis, except where noted. Data are expressed as mean ± SEM unless indicated otherwise, and n represents the number of neurons recorded. Two-sample paired Student t tests were used for comparison between 2 dependent groups, and 2-sample unpaired Student t tests were used for comparison between 2 independent groups. Wilcoxon signed rank tests were used for 2 dependent groups when the normality test failed using Shapiro-Wilk tests; for all pairwise differences tested using Student

t test, $P \geq 0.110$. One-way analysis of variance with post hoc of Bonferroni correction was used to compare >2 groups. For all the cases, $P < 0.05$ was considered as statistically significant.

RESULTS
Lidocaine Inhibits *I$_h$* in SG Neurons

As shown at the bottom of Figure 1A, I_h currents were evoked by hyperpolarizing voltage steps from −60 to −130 mV in 10-mV increments (1-second duration) from a holding potential of −50 mV. Lidocaine (100 μM) dramatically decreased I_h

(Fig. 1A). To test whether the currents recorded in our study were HCN channel mediated, we further applied ZD7288 (10 μM; 7 minutes) to the same neuron. ZD7288 reduced the current amplitude from 319 ± 64 to 19 ± 4 pA ($n = 10$ neurons from 8 rats; $P = 0.001$, paired t test), showing an inhibition of approximately 93% relative to the control. This result demonstrates that the current recorded in our study was produced by the HCN channel. To investigate the time course of I_h inhibition by lidocaine, we perfused lidocaine for 4 minutes. As illustrated in Figure 1D, the amplitude of the I_h currents decreased after lidocaine treatment, reaching a
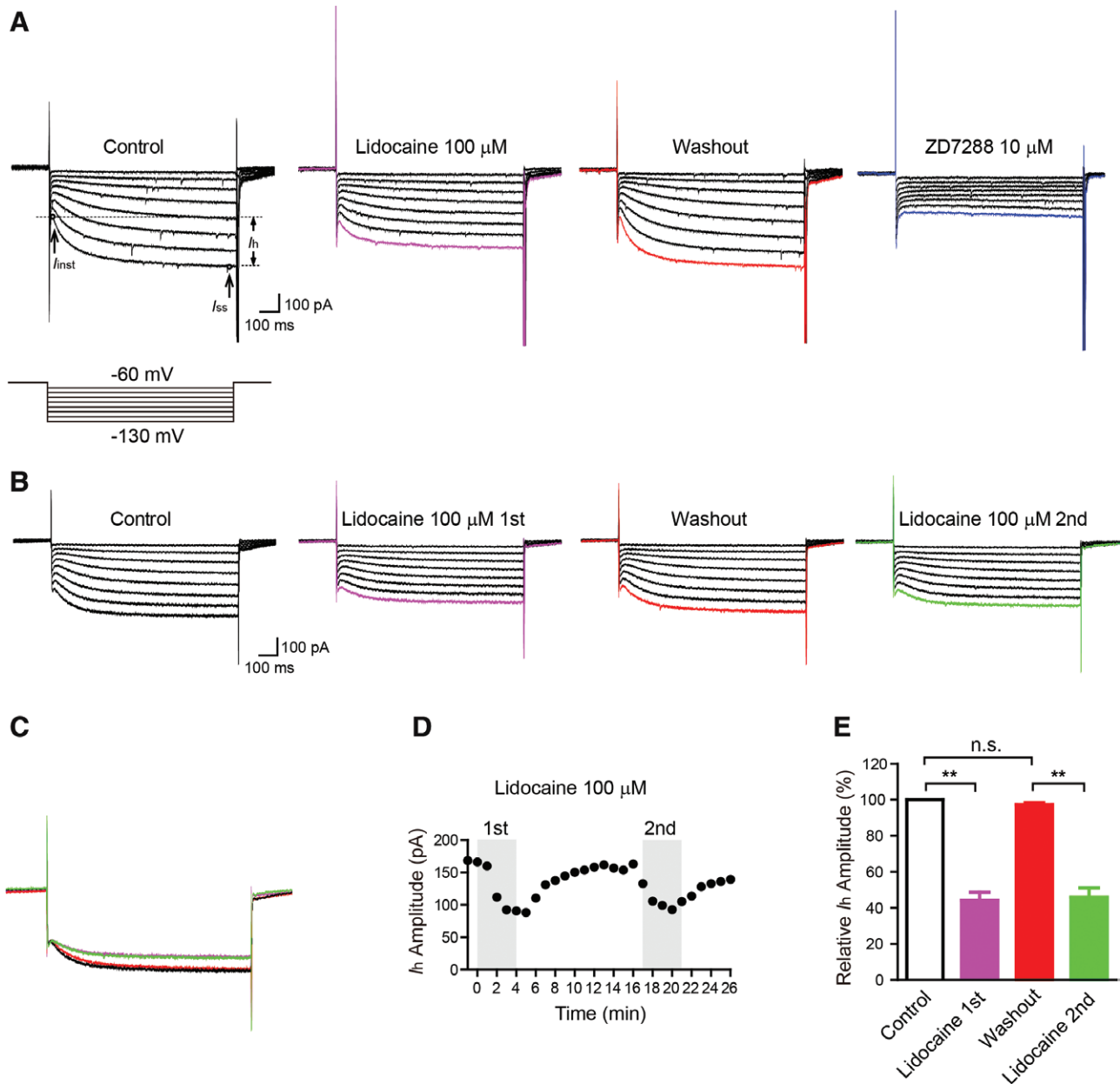
Figure 1. Lidocaine inhibits I_h in substantia gelatinosa neurons. A, Representative current responses to hyperpolarization voltage steps in the absence (control) and presence of lidocaine (100 μM), washout (recovery), and the following application of ZD7288 (10 μM) in a same neuron (upper). Lower panel shows the I_h evoking voltage protocol. Open circles in the lowest I_h trace indicate the instantaneous (I_{inst}) and steady state (I_{ss}) of I_h at −130 mV. B, Sample traces under control condition, the first perfusion of lidocaine (100 μM), washout, and the second perfusion of lidocaine. C, Superimposed traces of I_h (at −130 mV) in (B). D, Time course of the inhibition of lidocaine on I_h amplitude recorded from the same neuron in (B). Gray bars represent the periods of bath application of lidocaine. E, Summary data showing the percentage change in the peak I_h amplitude after application of lidocaine. In this and the following figures, *$P < 0.05$, **$P < 0.01$, ***$P < 0.001$. n.s. = no significant difference.

maximal level within 3 to 4 minutes and gradually returned to the control level in 5 to 6 minutes after washout without apparent rundown (Fig. 1, A and D). Thus, in this study, we perfused lidocaine for 4 minutes, and the amplitude of I_h under the action of lidocaine was measured after 4 ± 1 minutes.

To investigate whether desensitization is involved in lidocaine-induced inhibition of I_h, we applied lidocaine twice to the same neuron (Fig. 1B). The amplitude of I_h was significantly reduced to $44\% \pm 5\%$ that of the control ($n = 6$ neurons from 6 rats; 146 ± 22 pA; $P = 0.007$, 1-way analysis of variance with post hoc of Bonferroni) and recovered to $97\% \pm 1\%$ (143 ± 23 pA; $P = 0.911$) after washout (Fig. 1, B and E). When applying lidocaine to the same neuron once again, I_h was still reduced to $46\% \pm 6\%$ that of the control ($P = 0.009$). No significant difference in the I_h currents was observed between the 2 perfusions of lidocaine ($P = 0.976$; Fig. 1, C and E). This finding suggests that lidocaine markedly reduces I_h in the SG neurons, and the effect is rapid, reversible, and nondesensitized.

Lidocaine-Induced I_h Inhibition Is Not Mediated by Sodium Channels

To examine whether sodium channels could affect lidocaine's inhibition of I_h, we compared the I_h alterations under the coapplication of 0.5 μM TTX and 100 μM lidocaine (Fig. 2, A and B). Lidocaine still inhibited the amplitude of I_h to $52\% \pm 3\%$ ($n = 9$ neurons from 4 rats) that of the control (221 ± 62 pA; $P = 0.005$, paired t test, Fig. 2, A–D) in the presence of TTX, which was not significantly ($P = 0.193$, unpaired t test, Fig. 2F) different from the inhibition of I_h caused by lidocaine alone ($n = 22$ neurons from 11 rats; $47\% \pm 2\%$ that of the control) (296 ± 37 pA; $P < 0.0001$; paired t test, Fig. 2E). These data confirm that lidocaine directly blocks HCN channels without the involvement of TTX-sensitive voltage-gated sodium channels.

Lidocaine Inhibits I_h in SG Neurons in Concentration-Dependent Manner

To determine IC$_{50}$ for the inhibitory effect of lidocaine on I_h, we perfused lidocaine in increasing concentrations (1–1000 μM).
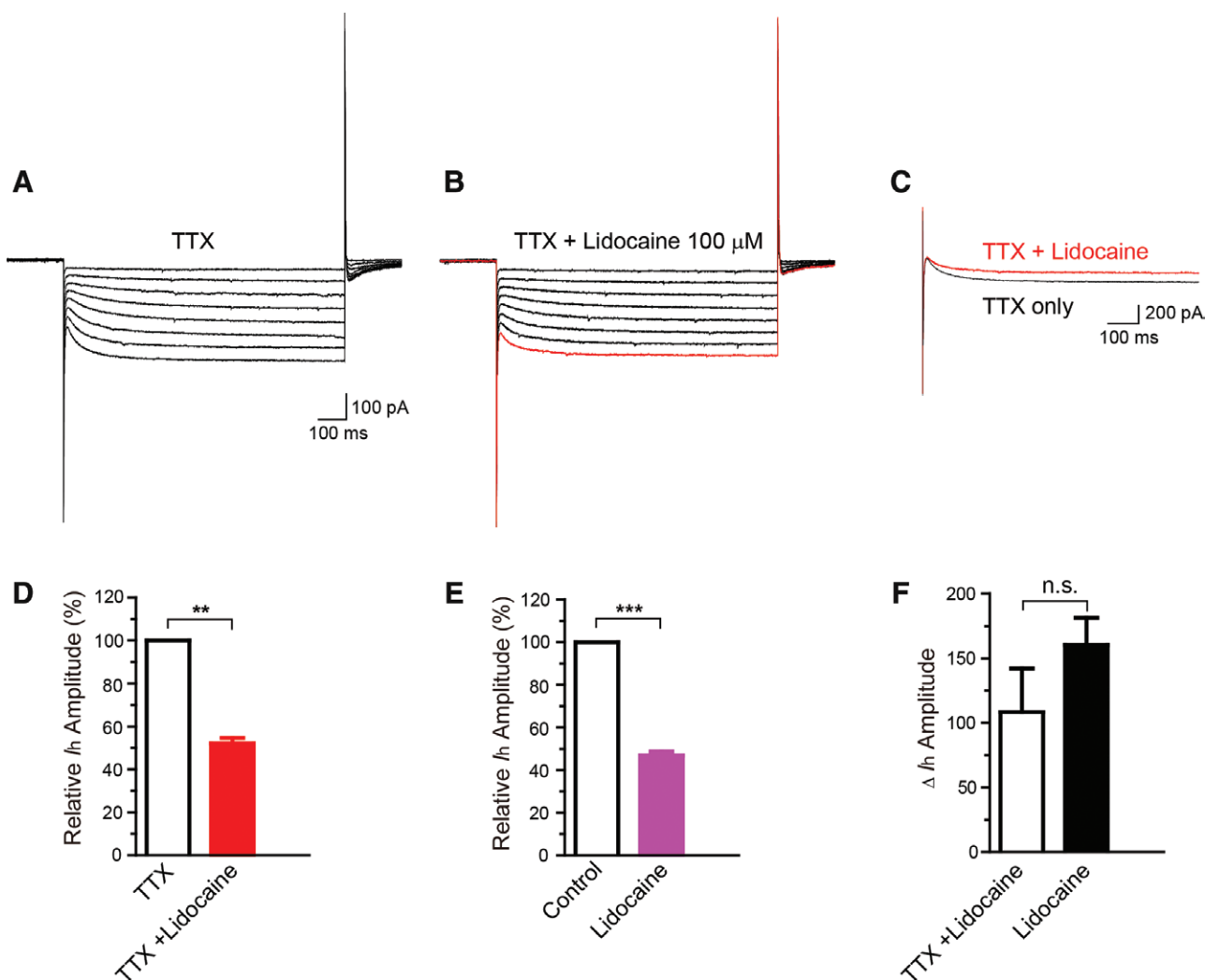
Figure 2. Lidocaine-induced I_h inhibition is not affected by tetrodotoxin (TTX). A and B, In the presence of TTX (0.5 μM) in artificial cerebrospinal fluid solution, lidocaine (100 μM) still decreased the peak amplitude of I_h. C, Superimposed traces of I_h (at −130 mV) recorded in (A and B). D and E, Averaged percentage of I_h inhibition by lidocaine in the presence and absence of TTX, respectively. F, Differences of I_h amplitude under the treatment of lidocaine in the presence and absence of TTX. In this and the other figures, *$P < 0.05$, **$P < 0.01$, ***$P < 0.001$.
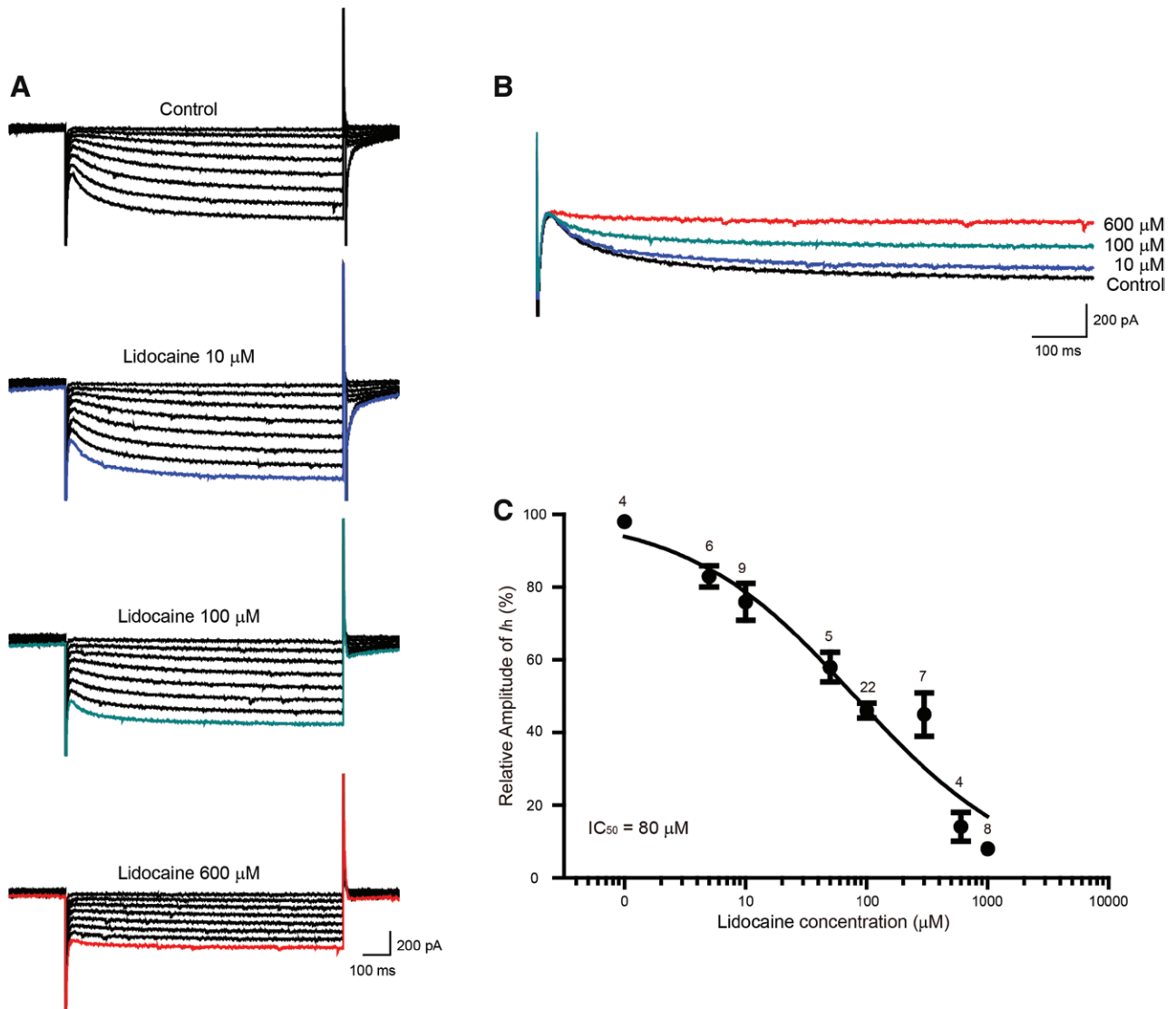
Figure 3. Lidocaine blocks I_h in substantia gelatinosa neurons in a concentration-dependent manner. A, Example traces before and after bath application of increasing concentrations of lidocaine (in micromolar): 10, 100, and 600, which are from the same neuron. B, Superimposed traces of I_h (at −130 mV) recorded in (A). C, Dose-response curve for I_h amplitude under the effect of lidocaine. The values in parentheses indicate the number of cells examined.

As illustrated in Figure 3, lidocaine inhibited I_h in a dose-dependent manner (IC_{50} = 80 µM and Hill coefficient = 0.63).

Lidocaine Shifts I_h Activation Curve to More Hyperpolarized Potential

To investigate whether lidocaine modifies the kinetics of HCN channels, I_h activation currents were evoked by the protocol shown at the bottom of Figure 4A. Both I_h and tail currents were significantly decreased by lidocaine (Fig. 4, A–C). The activation curves were plotted using the Boltzmann equation under the control conditions and during the perfusion of 600 µM lidocaine (Fig. 4D). Lidocaine significantly shifted $V_{0.5}$ toward more negative values from −109.7 ± 0.9 to −114.9 ± 1.1 mV, a shift of −5.2 mV (n = 23 neurons from 6 rats; P < 0.0001, paired t test; Fig. 4D and Table 1). Moreover, lidocaine significantly decreased the current density by 55% to 73% relative to that measured for the control neurons over the voltage range of −70 to −130

mV (n = 18 neurons from 6 rats; Fig. 4E and Table 1). As shown in Figure 4F, lidocaine increased the time constant to 127% to 148% that of the control (n = 19 neurons from 6 rats). For example, at −130 mV, the time constant was significantly lower in the presence of lidocaine (91.4 ± 9.2 milliseconds) than that of the control (69.8 ± 3.2 milliseconds; P = 0.003, paired t test; Fig. 4F and Table 1).

Lidocaine Shifts the Reversal Potential of I_h Current to More Negative Values

To further examine the effects of lidocaine on V_{rev} of I_h, we ran the protocol shown at the bottom of Figure 5A. After the bath application of lidocaine (600 µM), the magnitudes of the tail currents were clearly reduced (Fig. 5, A–C). The I-V curves were plotted by recording the tail currents in 24 SG neurons (Fig. 5D). The values of V_{rev} were −31.1 ± 1.3 and −38.6 ± 1.1 mV in the absence and presence of lidocaine, respectively (P < 0.0001, paired t test).
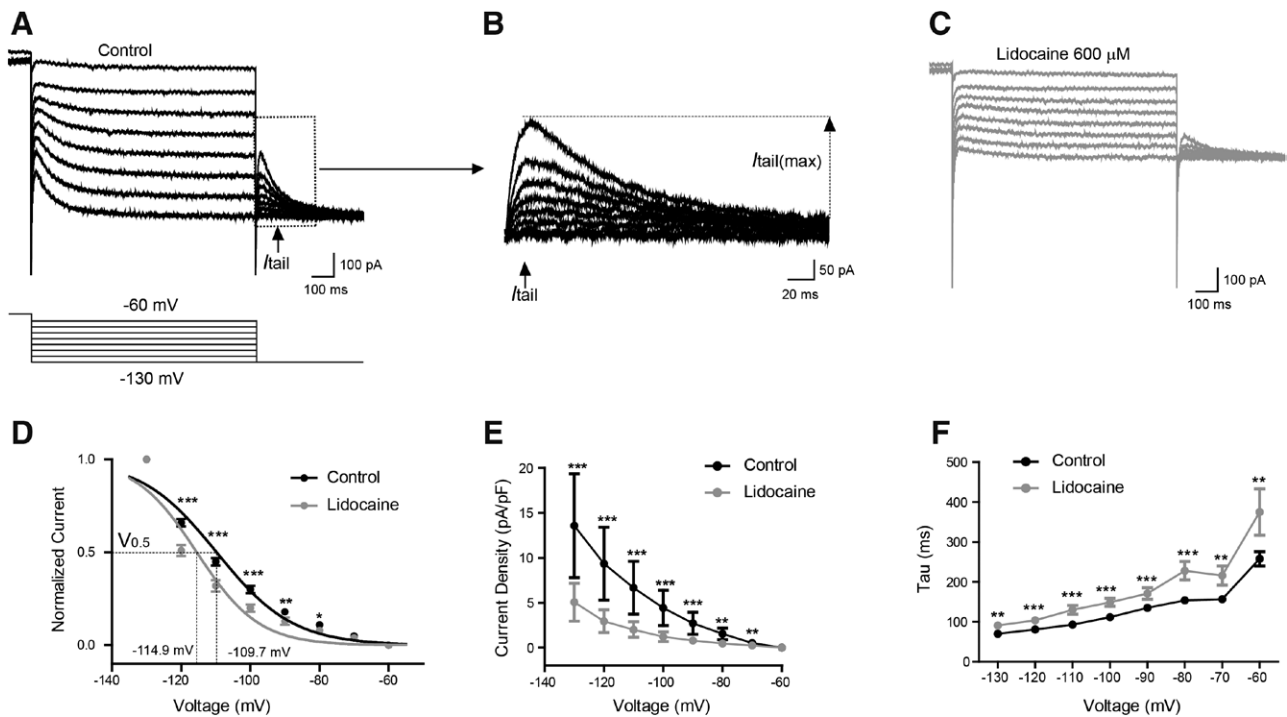
Figure 4. Lidocaine shifts I_h activation to more hyperpolarized potentials in substantia gelatinosa neurons. A, Control activation of I_h current (top) responses to the evoking protocol by hyperpolarizing voltage steps over the range from −60 to −130 mV in 10-mV increments for 1 s from the holding potential of −50 mV, which were then subjected to a voltage jump to −130 mV to obtain full activation (bottom). B, Enlargement of the tail currents in the rectangle shown in (A). Tail currents (marked as the arrow) were normalized to the maximum values $[(I_{tail, max} − I_{tail})/I_{tail, max}]$ to plot the activation curve shown in (D). C, Lidocaine markedly decreased the amplitude of tail currents (same neuron in A). D, Lidocaine clearly shifted $V_{0.5}$ to more negative values. E, Plot of I_h current density against the membrane potentials. Lidocaine reduced the current density from −70 to −130 mV. F, Time constant (τ) of I_h activation against the membrane potentials. Lidocaine significantly increased τ from −60 to −130 mV. In this and the other figures, *$P < 0.05$, **$P < 0.01$, ***$P < 0.001$.

Table 1. Effects of Lidocaine on HCN Channels' Kinetics of Activation in SG Neurons

Potential (mV)	Control			Lidocaine		
	Normalized current (%)	Current density (pA/pF)	Time constant (ms)	Normalized current (%)	Current density (pA/pF)	Time constant (ms)
−60	0	0	237 ± 20	0	0	397 ± 54 $P = 0.002$
−70	5 ± 1	0.5 ± 0.2	151 ± 9	4 ± 1 $P = 0.176$	0.2 ± 0.1 $P = 0.001$	223 ± 23 $P = 0.001$
−80	11 ± 1	1.5 ± 0.7	154 ± 8	8 ± 1 $P = 0.046$	0.5 ± 0.2 $P = 0.003$	230 ± 23 $P < 0.0001$
−90	18 ± 1	2.7 ± 1.2	130 ± 7	13 ± 2 $P = 0.008$	0.8 ± 0.3 $P < 0.0001$	176 ± 13 $P < 0.0001$
−100	30 ± 2	4.4 ± 1.9	112 ± 5	20 ± 2 $P < 0.0001$	1.2 ± 0.5 $P < 0.0001$	150 ± 9 $P < 0.0001$
−110	45 ± 2	6.7 ± 2.9	93 ± 4	32 ± 3 $P < 0.0001$	2.0 ± 0.9 $P < 0.0001$	131 ± 10 $P < 0.0001$
−120	66 ± 2	9.4 ± 4.1	80 ± 3	51 ± 3 $P < 0.0001$	3.0 ± 1.3 $P < 0.0001$	105 ± 7 $P < 0.0001$
−130	100	13.6 ± 5.8	70 ± 3	100	5.1 ± 2.1 $P < 0.0001$	91 ± 9 $P = 0.003$

Summarized data are the normalized currents, current densities, and time constants of SG neurons before and after application of lidocaine at a series of test potentials. Wilcoxon signed rank tests were used for the comparisons of normalized current and current density. Paired *t* tests were used for the comparisons of time constant. HCN = hyperpolarization-activated cyclic nucleotide.

Lidocaine Suppresses Burst Firing in SG Neurons

To investigate the effects of lidocaine on firing properties, voltage responses to the current injections were recorded in a current-clamp mode by using the protocol shown at the bottom of Figure 6C, which generates both action potential firing and a rebound spike.[17,48] Lidocaine at each concentration tested (100, 600, and 1000 μM) largely decreased the frequency of action potential firing (Fig. 6, A–C, left). In addition, lidocaine prolonged the latency of the rebound depolarization (Fig. 6D and Table 2) and decreased the rebound spike frequencies (Fig. 6E and Table 2). As shown in Figure 6F and Table 2, the variation of RMP toward hyperpolarization increased with
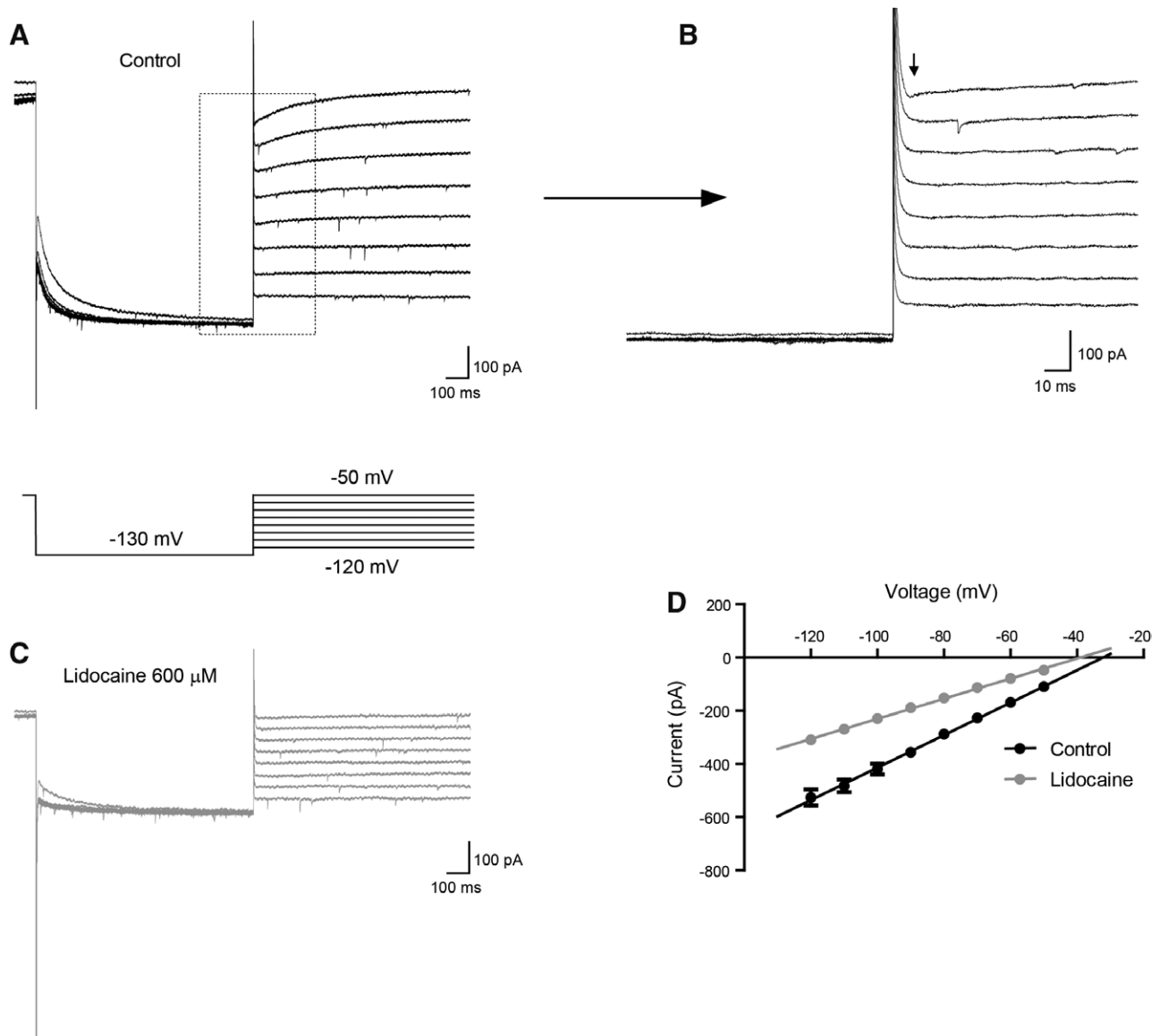
Figure 5. Lidocaine shifts the reversal potential of I_h current to more negative values in substantia gelatinosa neurons. A, Sample control traces of the deactivation of I_h current (top) and the evoking protocol (bottom: the membrane potential was stepped to −130 mV for 1 s from the holding potential of −50 mV to fully activate I_h, followed by a series of depolarization test potentials from −120 to −50 mV in 10-mV increments). B, The expanded traces of the tail currents in the rectangle shown in (A). Tail currents (marked as arrow) were measured at the onset of the test potentials. C, Lidocaine greatly reduced the amplitude of the tail currents (the same neuron in A); D, I-V curves constructed from the tail currents in the absence (black) and presence of lidocaine (gray) to each test potential. Lidocaine shifts the reversal potential to more negative values.

the concentration of lidocaine. In addition, lidocaine significantly increased R_{in} (Fig. 6G and Table 2).

I_h Expression Varies with SG Neuron Firing Pattern
To determine I_h expression in various types of SG neurons, action potentials were elicited with a depolarizing current (120 pA) injection with a duration of 1 second (Fig. 7, Aa–h). On the basis of previous studies,[39,40] we categorized SG neurons ($n = 102$) into the following 7 groups: tonic firing (63%), delayed firing (14%), single spike (10%), initial burst (8%), phasic firing (5%), gap firing (2%), and reluctant firing (2%) neurons (Fig. 7A). Among these groups of neurons, 64% of tonic-firing neurons, 21% of delayed-firing neurons, 70% of

single-spike neurons, 63% of initial-burst neurons, 50% of phasic-firing neurons, 100% of gap-firing neurons and no reluctant-firing neurons were recorded with I_h (Fig. 7B). Conversely, HCN channels consisted of 4 subtypes with different time constants.[49] To roughly examine the HCN channel subtypes in SG neurons, we measured the time constant of I_h at −130 mV, which ranged from 49 to 1289 milliseconds ($n = 51$; 231 ± 40 milliseconds), with most values being <400 milliseconds (Fig. 7C). These results suggest that most of the HCN channels in SG are probably HCN1 and HCN2 like.

DISCUSSION
In this study, we demonstrated that lidocaine strongly and rapidly blocks I_h in SG neurons of the spinal dorsal horn
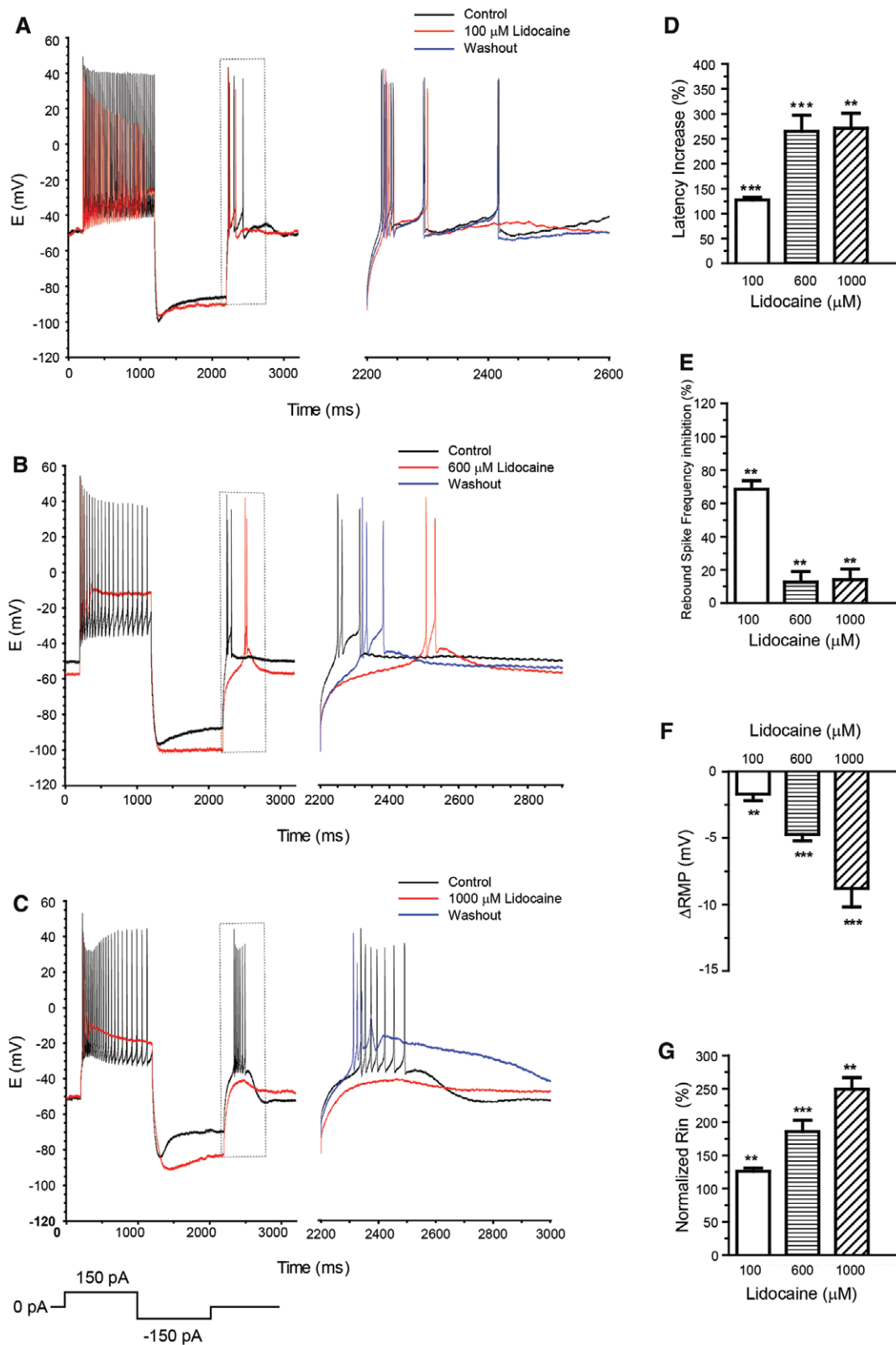
Figure 6. The effect of lidocaine on firing properties in substantia gelatinosa neurons. A–C (left), Voltage responses to the current commands shown at the bottom during control (black), and the administration of different concentrations of lidocaine (red): 100, 600, and 1000 μM, respectively. Right, Enlargement of rectangular areas shown in (A–C), with a trace of recovery after washout (blue). Lidocaine reduced the frequency of sodium-dependent action potentials and the rebound firings and increased the latency of the rebound firings. Bottom, Voltage responses were recorded under a 1-s depolarization current pulse from 0 to 150 pA, followed by a 1-s hyperpolarization current pulse from 0 to −150 pA. D–G, Grouped data show the percentage change in rebound depolarization latency, frequency, resting membrane potential (RMP) changes, and R_{in} after application of different concentrations of lidocaine. In this and the other figures, $*P < 0.05$, $**P < 0.01$, $***P < 0.001$.

Table 2. Effects of Lidocaine on Latency and Frequency of RD, RMP, and Rin in SG Neurons

Control					Lidocaine			
RD latency (ms)	RD frequency (Hz)	RMP (mV)	R$_{in}$ (MΩ)	Concentration	RD latency (ms)	RD frequency (Hz)	RMP (mV)	R$_{in}$ (MΩ)
32.6 ± 2.7 (n = 22 from 6 rats)	7.5 ± 1.1 (n = 11 from 4 rats)	−49.4 ± 0.8 (n = 14 from 6 rats)	193 ± 18 (n = 19 from 10 rats)	100 μM	41.0 ± 3.6 $P < 0.0001$	5.1 ± 0.8 $P = 0.005$	−51.1 ± 0.8 $P = 0.003$	244 ± 29 $P = 0.002$
31.4 ± 4.7 (n = 17 from 6 rats)	3.2 ± 1.1 (n = 13 from 6 rats)	−52.7 ± 0.9 (n = 11 from 6 rats)	191 ± 32 (n = 10 from 6 rats)	600 μM	79.5 ± 18 $P < 0.0001$	0.8 ± 0.4 $P = 0.001$	−57.5 ± 1.0 $P < 0.0001$	343 ± 51 $P < 0.0001$
50.5 ± 9.7 (n = 14 from 7 rats)	4.8 ± 1.2 (n = 11 from 7 rats)	−54.6 ± 1.9 (n = 10 from 7 rats)	235 ± 38 (n = 10 from 4 rats)	1000 μM	119.0 ± 18.3 ($P = 0.001$)	0.9 ± 0.4 $P = 0.003$	−63.4 ± 1.9 $P < 0.0001$	574 ± 100 $P = 0.001$

Summarized data are the latency and frequency of RD, RMP, and input resistance (R$_{in}$) of SG neurons before and after application of increasing concentrations of lidocaine. Wilcoxon signed rank tests were used for the comparisons of RD latency and frequency. Paired t tests were used for the comparisons of RMP and R$_{in}$. RD = rebound depolarization; RMP = resting membrane potential; SG = substantia gelatinosa.
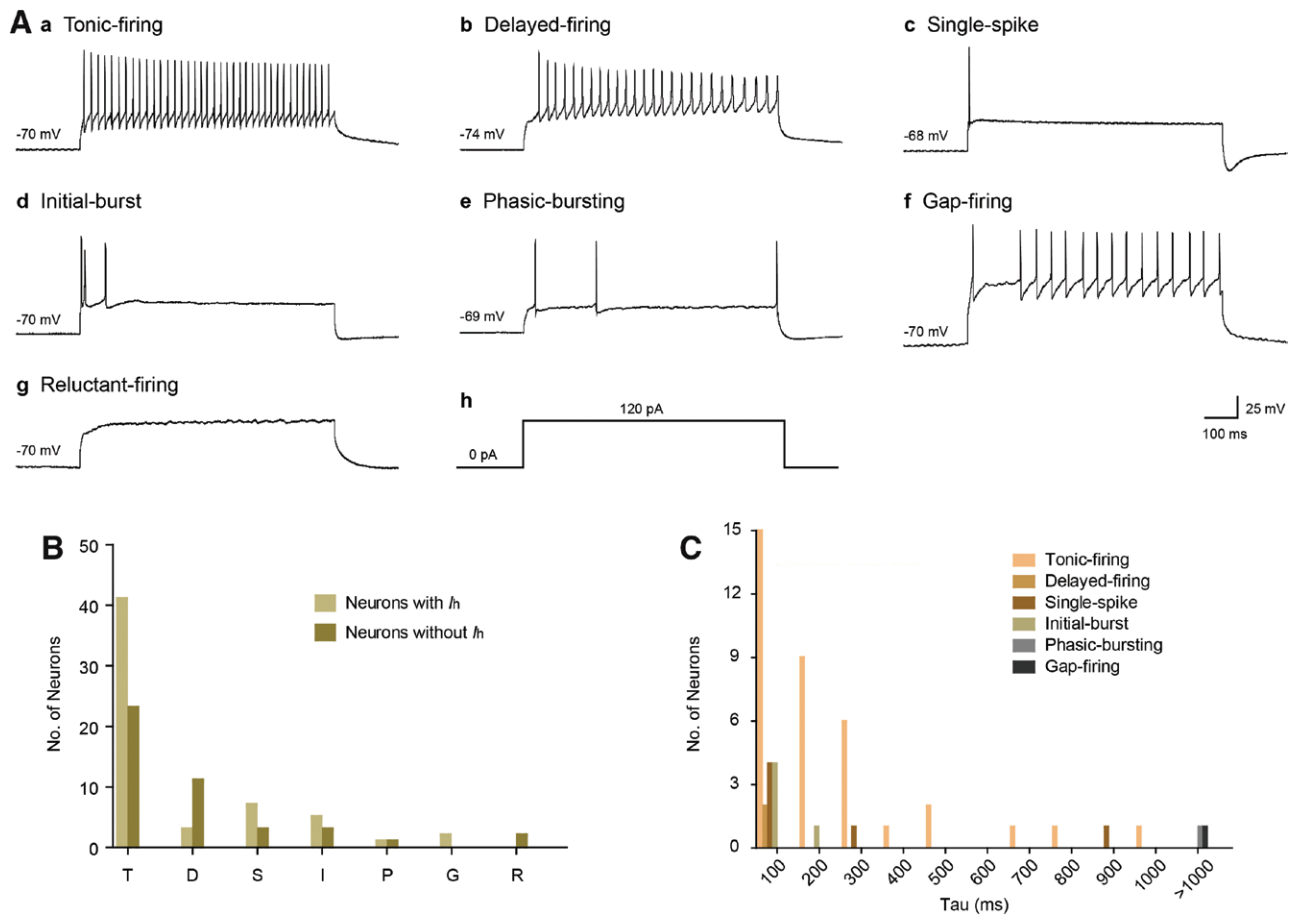
Figure 7. I$_h$ expression in different firing patterns of substantia gelatinosa (SG) neurons. A, Representative firing patterns in SG neurons: tonic-firing (a), delayed-firing (b), single-spike (c), initial-burst (d), phasic-bursting (e), gap-firing (f), and reluctant-firing (g) neurons evoked by the protocol in (h). B, Summary bar graph showing numbers of neurons expressing I$_h$ with respect to cell electrophysiologic classification. C, Histogram figure showing τ values (at −130 mV) in the subtypes of SG neurons.

in a reversible and concentration-dependent manner. Our results show that lidocaine could downregulate the excitability of SG neurons by inhibiting HCN currents, providing new insight into the mechanism underlying the analgesic effect of lidocaine.

It is generally believed that sodium channels are the main target of local anesthetics, including lidocaine. By blocking sodium channels, lidocaine inhibits action potential propagation and neuronal excitability. Recently, lidocaine was found to block HCN channels in oocytes and HEK 293 cells,[18] DRG neurons,[16,19] and thalamocortical neurons.[17] In this study, we demonstrated for the first time that lidocaine can decrease the amplitude of I$_h$ in SG neurons. The concentrations of lidocaine used in our study are clinically relevant to spinal and epidural anesthesia, without being toxic to the cardiovascular or central nervous systems.[50] The

maximal blocking effect of lidocaine on the amplitude of I_h in SG neurons was approximately 92%, indicating a high efficacy of lidocaine toward HCN channels. In addition, lidocaine-induced I_h inhibition was not affected by TTX. It has been reported that voltage-gated sodium channels in laminae I/II cells of the spinal cord are primarily TTX-sensitive isoforms.[51] Thus, it is clear that sodium channels are not involved in lidocaine-induced I_h inhibition.

Ion channel activation is an important aspect of channel kinetics. The negative shift of I_h activation would decrease the probability that HCN channels are open in the resting state and thus decrease neuronal excitability. In this study, we found that the I_h activation curve is shifted toward negative values by lidocaine. Meng et al.[18] also reported that, in HEK 293 cells, lidocaine could negatively shift I_h activation for homomeric HCN1 channels or heteromeric HCN1 to HCN2 channels. The time constant is another key issue associated with channel kinetics. The speed of HCN channel activation decreases with an increasing time constant. Consistent with its action on the I_h activation curve, lidocaine increased the time constant of I_h at all test potentials in SG neurons.

V_{rev} is determined by ion channel selectivity. HCN channel opening allows for a greater influx of Na^+ and a lower efflux of K^+, with a net inward current.[20] Theoretically, the V_{rev} value of HCN channels can be calculated by using the Goldman-Hodgkin-Katz equation. However, unlike that of cloned cells, the exact ratio of Na^+/K^+ permeability through HCN channels could not be determined in slice preparations because the distribution of HCN channel subtypes in different cell types is not the same. Therefore, in this and our previous studies,[41] the x-intercept of the I_h I-V curve is represented as V_{rev}. Lidocaine shifted the V_{rev} value of HCN channels from −31.1 to −38.6 mV in SG neurons, which resembles the effect of bupivacaine on HCN channels in DRG.[19] Such an effect corresponds to altered Na^+ and K^+ selectively of HCN channels. Alternately, effects on background currents could be responsible for the apparent alteration of V_{rev}.

In the nervous system, rebound depolarization plays a pivotal role in neuronal excitability.[52,53] The latency of rebound depolarization is determined by I_h.[54] In our study, lidocaine not only delayed the latency of rebound depolarization but also reduced the number of rebound spikes, in line with previous studies on thalamocortical neurons.[5,17,55] These data further indicate that lidocaine can suppress the excitability of SG neurons by blocking HCN channels.

Previous studies have shown that lidocaine can regulate the resting properties of neurons.[16,17] Similarly, in this study, lidocaine markedly blocked HCN channels in SG neurons, causing the RMP to more hyperpolarized voltages. In addition, R_{in} increased significantly with the concentration of lidocaine from 100 to 1000 μM in our study.

The composition of SG neurons is complex and has not been clearly elucidated to date. Our data show that I_h can be recorded for approximately 58% of SG neurons. Among these neurons, tonic-firing cells have the highest expression level (64%). It has been reported that most tonic-firing SG neurons are excitatory interneurons.[38] Therefore, the blocking of I_h by lidocaine may lead to the inhibition of SG neuron excitability. In addition, most of the time constants of the

I_h currents we recorded here were <400 milliseconds, suggesting higher contents of the HCN1 and HCN2 subtypes in SG neurons. Further experiments, such as immunohistochemistry and single-cell reverse transcription polymerase chain reaction, are required to obtain the exact distribution of HCN channel subtypes in SG neurons.

Taken together, our results demonstrate that lidocaine is an effective blocker of HCN channels in SG neurons. This inhibition may downregulate the excitability of SG neurons by decreasing the rebound depolarization frequency and prolonging rebound depolarization latency. Given that SG neurons play crucial roles in pain modulation, our observations may suggest a novel cellular mechanism underlying the analgesic effects of lidocaine in spinal fluid. ▪

REFERENCES
1. Smith LJ, Bentley E, Shih A, Miller PE. Systemic lidocaine infusion as an analgesic for intraocular surgery in dogs: a pilot study. Vet Anaesth Analg 2004;31:53–63
2. McCarthy GC, Megalla SA, Habib AS. Impact of intravenous lidocaine infusion on postoperative analgesia and recovery from surgery: a systematic review of randomized controlled trials. Drugs 2010;70:1149–63

3. Vigneault L, Turgeon AF, Côté D, Lauzier F, Zarychanski R, Moore L, McIntyre LA, Nicole PC, Fergusson DA. Perioperative intravenous lidocaine infusion for postoperative pain control: a meta-analysis of randomized controlled trials. Can J Anaesth 2011;58:22–37

4. Butterworth JF, Strichartz GR. Molecular mechanisms of local anesthesia: a review. Anesthesiology 1990;72:711–34

5. Schwarz SK, Puil E. Analgesic and sedative concentrations of lignocaine shunt tonic and burst firing in thalamocortical neurones. Br J Pharmacol 1998;124:1633–42

6. Xiong Z, Strichartz GR. Inhibition by local anesthetics of Ca2+ channels in rat anterior pituitary cells. Eur J Pharmacol 1998;363:81–90

7. Lee YS, Maruyama M, Chang PC, Park HW, Rhee KS, Hsieh YC, Hsueh CH, Shen C, Lin SF, Hwang HS, Yin H, Knollmann BC, Chen PS. Ryanodine receptor inhibition potentiates the activity of Na channel blockers against spontaneous calcium elevations and delayed afterdepolarizations in Langendorff-perfused rabbit ventricles. Heart Rhythm 2012;9:1125–32

8. Olschewski A, Hempelmann G, Vogel W, Safronov BV. Blockade of Na+ and K+ currents by local anesthetics in the dorsal horn neurons of the spinal cord. Anesthesiology 1998;88:172–9

9. Komai H, McDowell TS. Local anesthetic inhibition of voltage-activated potassium currents in rat dorsal root ganglion neurons. Anesthesiology 2001;94:1089–95

10. Kindler CH, Paul M, Zou H, Liu C, Winegar BD, Gray AT, Yost CS. Amide local anesthetics potently inhibit the human tandem pore domain background K+ channel TASK-2 (KCNK5). J Pharmacol Exp Ther 2003;306:84–92

11. Wolff M, Schnöbel-Ehehalt R, Mühling J, Weigand MA, Olschewski A. Mechanisms of lidocaine's action on subtypes of spinal dorsal horn neurons subject to the diverse roles of Na(+) and K(+) channels in action potential generation. Anesth Analg 2014;119:463–70

12. Piao LH, Fujita T, Jiang CY, Liu T, Yue HY, Nakatsuka T, Kumamoto E. TRPA1 activation by lidocaine in nerve terminals results in glutamate release increase. Biochem Biophys Res Commun 2009;379:980–4

13. Leffler A, Lattrell A, Kronewald S, Niedermirtl F, Nau C. Activation of TRPA1 by membrane permeable local anesthetics. Mol Pain 2011;7:62

14. Binshtok AM, Bean BP, Woolf CJ. Inhibition of nociceptors by TRPV1-mediated entry of impermeant sodium channel blockers. Nature 2007;449:607–10

15. Leng TD, Lin J, Sun HW, Zeng Z, O'Bryant Z, Inoue K, Xiong ZG. Local anesthetic lidocaine inhibits TRPM7 current and TRPM7-mediated zinc toxicity. CNS Neurosci Ther 2015;21:32–9

16. Zhou C, Ke B, Zhao Y, Liang P, Liao D, Li T, Liu J, Chen X. Hyperpolarization-activated cyclic nucleotide-gated channels may contribute to regional anesthetic effects of lidocaine. Anesthesiology 2015;122:606–18

17. Putrenko I, Schwarz SK. Lidocaine blocks the hyperpolarization-activated mixed cation current, I(h), in rat thalamocortical neurons. Anesthesiology 2011;115:822–35

18. Meng QT, Xia ZY, Liu J, Bayliss DA, Chen X. Local anesthetic inhibits hyperpolarization-activated cationic currents. Mol Pharmacol 2011;79:866–73

19. Bischoff U, Bräu ME, Vogel W, Hempelmann G, Olschewski A. Local anaesthetics block hyperpolarization-activated inward current in rat small dorsal root ganglion neurones. Br J Pharmacol 2003;139:1273–80

20. Biel M, Wahl-Schott C, Michalakis S, Zong X. Hyperpolarization-activated cation channels: from genes to function. Physiol Rev 2009;89:847–85

21. Postea O, Biel M. Exploring HCN channels as novel drug targets. Nat Rev Drug Discov 2011;10:903–14

22. Ludwig A, Herrmann S, Hoesl E, Stieber J. Mouse models for studying pacemaker channel function and sinus node arrhythmia. Prog Biophys Mol Biol 2008;98:179–85

23. Atherton JF, Kitano K, Baufreton J, Fan K, Wokosin D, Tkatch T, Shigemoto R, Surmeier DJ, Bevan MD. Selective participation of somatodendritic HCN channels in inhibitory but not excitatory synaptic integration in neurons of the subthalamic nucleus. J Neurosci 2010;30:16025–40

24. Noam Y, Bernard C, Baram TZ. Towards an integrated view of HCN channel role in epilepsy. Curr Opin Neurobiol 2011;21:873–9

25. Kase D, Imoto K. The role of HCN channels on membrane excitability in the nervous system. J Signal Transduct 2012;2012:619747

26. Chaplan SR, Guo HQ, Lee DH, Luo L, Liu C, Kuei C, Velumian AA, Butler MP, Brown SM, Dubin AE. Neuronal hyperpolarization-activated pacemaker channels drive neuropathic pain. J Neurosci 2003;23:1169–78

27. Yao H, Donnelly DF, Ma C, LaMotte RH. Upregulation of the hyperpolarization-activated cation current after chronic compression of the dorsal root ganglion. J Neurosci 2003;23:2069–74

28. Jiang YQ, Xing GG, Wang SL, Tu HY, Chi YN, Li J, Liu FY, Han JS, Wan Y. Axonal accumulation of hyperpolarization-activated cyclic nucleotide-gated cation channels contributes to mechanical allodynia after peripheral nerve injury in rat. Pain 2008;137:495–506

29. Jiang YQ, Sun Q, Tu HY, Wan Y. Characteristics of HCN channels and their participation in neuropathic pain. Neurochem Res 2008;33:1979–89

30. Lee DH, Chang L, Sorkin LS, Chaplan SR. Hyperpolarization-activated, cation-nonselective, cyclic nucleotide-modulated channel blockade alleviates mechanical allodynia and suppresses ectopic discharge in spinal nerve ligated rats. J Pain 2005;6:417–24

31. Dalle C, Eisenach JC. Peripheral block of the hyperpolarization-activated cation current (Ih) reduces mechanical allodynia in animal models of postoperative and neuropathic pain. Reg Anesth Pain Med 2005;30:243–8

32. Momin A, Cadiou H, Mason A, McNaughton PA. Role of the hyperpolarization-activated current Ih in somatosensory neurons. J Physiol 2008;586:5911–29

33. Orio P, Madrid R, de la Peña E, Parra A, Meseguer V, Bayliss DA, Belmonte C, Viana F. Characteristics and physiological role of hyperpolarization activated currents in mouse cold thermoreceptors. J Physiol 2009;587:1961–76

34. Emery EC, Young GT, Berrocoso EM, Chen L, McNaughton PA. HCN2 ion channels play a central role in inflammatory and neuropathic pain. Science 2011;333:1462–6

35. Kroin JS, Buvanendran A, Beck DR, Topic JE, Watts DE, Tuman KJ. Clonidine prolongation of lidocaine analgesia after sciatic nerve block in rats is mediated via the hyperpolarization-activated cation current, not by alpha-adrenoreceptors. Anesthesiology 2004;101:488–94

36. Brummett CM, Hong EK, Janda AM, Amodeo FS, Lydic R. Perineural dexmedetomidine added to ropivacaine for sciatic nerve block in rats prolongs the duration of analgesia by blocking the hyperpolarization-activated cation current. Anesthesiology 2011;115:836–43

37. Maxwell DJ, Belle MD, Cheunsuang O, Stewart A, Morris R. Morphology of inhibitory and excitatory interneurons in superficial laminae of the rat dorsal horn. J Physiol 2007;584:521–33

38. Santos SF, Rebelo S, Derkach VA, Safronov BV. Excitatory interneurons dominate sensory processing in the spinal substantia gelatinosa of rat. J Physiol 2007;581:241–54

39. Ruscheweyh R, Sandkühler J. Lamina-specific membrane and discharge properties of rat spinal dorsal horn neurones in vitro. J Physiol 2002;541:231–44

40. Yasaka T, Tiong SY, Hughes DI, Riddell JS, Todd AJ. Populations of inhibitory and excitatory interneurons in lamina II of the adult rat spinal dorsal horn revealed by a combined electrophysiological and anatomical approach. Pain 2010;151:475–88

41. Liu N, Zhang D, Zhu M, Luo S, Liu T. Minocycline inhibits hyperpolarization-activated currents in rat substantia gelatinosa neurons. Neuropharmacology 2015;95:110–20

42. Kawamata M, Furue H, Kozuka Y, Narimatsu E, Yoshimura M, Namiki A. Changes in properties of substantia gelatinosa neurons after surgical incision in the rat: in vivo patch-clamp analysis. Anesthesiology 2006;104:432–40

43. Lu Y, Dong H, Gao Y, Gong Y, Ren Y, Gu N, Zhou S, Xia N, Sun YY, Ji RR, Xiong L. A feed-forward spinal cord glycinergic neural circuit gates mechanical allodynia. J Clin Invest 2013;123:4050–62

44. Rateau Y, Ropert N. Expression of a functional hyperpolarization-activated current (Ih) in the mouse nucleus reticularis thalami. J Neurophysiol 2006;95:3073–85
45. Macri V, Accili EA. Structural elements of instantaneous and slow gating in hyperpolarization-activated cyclic nucleotide-gated channels. J Biol Chem 2004;279:16832–46
46. Gao LL, McMullan S, Djouhri L, Acosta C, Harper AA, Lawson SN. Expression and properties of hyperpolarization-activated current in rat dorsal root ganglion neurons with known sensory function. J Physiol 2012;590:4691–705
47. Yan H, Li Q, Fleming R, Madison RD, Wilson WA, Swartzwelder HS. Developmental sensitivity of hippocampal interneurons to ethanol: involvement of the hyperpolarization-activated current, Ih. J Neurophysiol 2009;101:67–83
48. Ries CR, Puil E. Mechanism of anesthesia revealed by shunting actions of isoflurane on thalamocortical neurons. J Neurophysiol 1999;81:1795–801
49. He C, Chen F, Li B, Hu Z. Neurophysiology of HCN channels: from cellular functions to multiple regulations. Prog Neurobiol 2014;112:1–23
50. Markey JR, Montiague R, Winnie AP. A comparative efficacy study of hyperbaric 5% lidocaine and 1.5% lidocaine for spinal anesthesia. Anesth Analg 1997;85:1105–7
51. Hildebrand ME, Mezeyova J, Smith PL, Salter MW, Tringham E, Snutch TP. Identification of sodium channel isoforms that mediate action potential firing in lamina I/II spinal cord neurons. Mol Pain 2011;7:67
52. Aizenman CD, Linden DJ. Regulation of the rebound depolarization and spontaneous firing patterns of deep nuclear neurons in slices of rat cerebellum. J Neurophysiol 1999;82:1697–709
53. McCormick DA, Pape HC. Properties of a hyperpolarization-activated cation current and its role in rhythmic oscillation in thalamic relay neurones. J Physiol 1990;431:291–318
54. Rivera-Arconada I, Lopez-Garcia JA. Characterisation of rebound depolarisation in mice deep dorsal horn neurons in vitro. Pflugers Arch 2015;467:1985–96
55. Schwarz SK, Puil E. Lidocaine produces a shunt in rat [correction of rats] thalamocortical neurons, unaffected by GABA(A) receptor blockade. Neurosci Lett 1999;269:25–8